Journal of Molecular Catalysis A: Chemical 316 (2010) 16–22

Contents lists available at ScienceDirect

Journal of Molecular Catalysis A: Chemical

journal homepage: www.elsevier.com/locate/molcata

Interstellar catalysis: Formation of small molecules on a graphitic flake

L.S. Rodríguez [a], F. Ruette [a,*], M. Sánchez [a], C. Mendoza [b]

[a] Centro de Química, Instituto Venezolano de Investigaciones Científicas (IVIC), PO Box 20632, Caracas 1020A, Venezuela
[b] Centro de Física, Instituto Venezolano de Investigaciones Científicas (IVIC), PO Box 20632, Caracas 1020A, Venezuela

ARTICLE INFO

Article history:
Received 4 May 2009
Received in revised form
10 September 2009
Accepted 18 September 2009
Available online 26 September 2009

PACS:
68.43. −h
82.65.+r

Keywords:
Semi-empirical models and model calculations
Models of surface chemistry reactions
Chemisorption
Molecular formation
Organic molecules
Polycyclic aromatic hydrocarbons

ABSTRACT

The formation of organic molecules of the type XH_n, where X is H, C, N and O and $n = 1 - 4$, on the hydrogenated surface of a polycyclic aromatic hydrocarbon flake (coronene) has been examined in detail with the CATIVIC parametric quantum chemical code. Hydrogen chemisorption on different sites, surface–adsorbate bonding properties and layer formation are studied. The interactions of H, O, N and C on one-center sites of the H-saturated monolayer give rise to the formation of free H_2, OH and NH while the CH molecule remains attached to the surface. Reactions on two-center sites lead to the formation of the free triatomic molecules H_2O, NH_2 and CH_2. One-center interactions of OH, NH, NH_2, CH_2 and CH_3 also result in the respective formation of H_2O, NH_2, NH_3, CH_3 and CH_4. We find that the reactions of atoms and small molecules with the hydrogenated coronene surface in most cases must overcome relatively high energy barriers in order to lead to reaction products.

1. Introduction

Molecular formation in the interstellar medium (ISM) is a topic of astrochemical interest and the possible starting point of life from extraterrestrial origins [1]. Organic molecules can be synthesized on dust grains built of nano- and micro-aggregates containing polycyclic aromatic hydrocarbons (PAHs) [2]. Experimental studies of ISM conditions are difficult because of the very low temperature and pressure and long reaction times. For this reason, quantum chemical modeling may be a useful tool in the understanding of molecular formation routes.

Atomic interactions with graphitic surfaces modeled with small PAHs have been previously explored using semi-empirical approaches [3–6], including the important surface formation of molecular hydrogen by the Eley–Rideal mechanism [7]. The astrochemical efficiency of the latter is supported by correlation between H_2 and PAH emissions in UV-dominated regions [8,9]. Hydrogen recombination on the graphitic surface has been confirmed with the density-functional-theory (DFT) approach and a smaller model ($C_{10}H_8^+ + H$) [10] and with anthracene and pyrene substrates [11]. The atomic hydrogen interactions on the central sites and edge of naphthalene, anthracene, pyrene and coronene cations have been examined with DFT and the spin projected MP2 (PMP2) methods, finding a very small activation energy for H abstraction during H_2 formation [12]. Chemisorption of C, N and O on different surface sites of PAH flakes, namely coronene ($C_{24}H_{12}$), has also been reported [13]. More recently, many DFT calculations have been carried out to study H adsorption, multiple adsorption, recombination, surface relaxation on graphite surfaces [14–26]. However, molecular formation on the hydrogenated graphite surface has not been treated which is relevant in the chemistry of interstellar grains since the latter are usually in an H-rich environment.

The assembly of larger organic molecules on PAH flakes (coronene and circumcoronene), e.g. amino acids (glycine and alanine), monocarboxylic acids and polyols, has been studied with parametric methods [27,28]. It has been found that polymer length is determined by the competition between surface diffusion and hydrogenation. Many of these molecules such as glycine, acetic acid and sugar have been reported in ISM observations [29–31].

* Corresponding author. Present address: Centro de Química, Instituto Venezolano de Investigaciones Científicas (IVIC), PO Box 21827, Caracas 1020A, Venezuela. Tel.: +58 212 504 1374; fax: +58 212 504 1350.
E-mail addresses: lsrodriguezt@gmail.com (L.S. Rodríguez), fruette@ivic.ve (F. Ruette), msanchez@ivic.ve (M. Sánchez), claudio@ivic.ve (C. Mendoza).

1381-1169/$ – see front matter © 2009 Elsevier B.V. All rights reserved.
doi:10.1016/j.molcata.2009.09.011

In the present work, we study the formation of the intermediate fragments involved in organic synthesis where H surface coverage is determinant. The CATIVIC parametric package [32], modified to explore surface processes such as docking and diffusion, has been employed. Potential energy curves are calculated, and several molecular and surface properties are analyzed in order to understand the formation and adsorption of diatomic, triatomic and multi-atomic molecules. A brief description of the bond strength method and surface models is presented in Section 2. Changes in hydrogen adsorption properties with coverage growth are discussed in Section 3, together with the formation of diatomic and triatomic molecules and their corresponding potential energy curves. Finally, comments and conclusions are summarized in Section 4.

2. Method and surface models

Calculations have been performed with a parametric method referred to as CATIVIC [32–34]. This code has been designed to model molecular reactions on surfaces, in particular the adsorbate–substrate interactions (adsorption process). In quantum parametric methods, elementary functionals representing the total energy are optimized so as to reproduce observed molecular geometries and energetic properties [35,36]. The parametric functionals used here are based on the MINDO/SR method [37] which is an extension of MINDO/3 [38] for transition metals. The program evaluates the bond strength (diatomic binding energy E_{AB}) in terms of the diatomic energy (ϵ_{AB}), monoatomic energies (ϵ_A and ϵ_B), Mulliken charge, Wiberg index (W) and the equilibrium interatomic distance (r_{AB}). Values of E_{AB} are obtained with the equation [39]

$$E_{AB} = \epsilon_{AB} + f_A^{AB}\epsilon_A + f_B^{AB}\epsilon_B \quad (1)$$

where ϵ_A is the monoatomic energy and

$$f_A^{AB} = \frac{\epsilon_{AB}}{\sum_{A>C}\epsilon_{AC}}, \quad (2)$$

subject to the condition that the total binding energy is given by

$$E_T = \sum_{A>B} E_{AB}. \quad (3)$$

Following earlier work [7,13,27,28], the selected surface model is a PAH flake, namely coronene (see Fig. 1). In the case of interstellar grains, this is believed to be an adequate surface model due to their multilayered structure and different degrees of porosity [40]. Although coronene is able to form aggregates [41], interactions between layers are weak, and therefore the effects of surface underlayers on atomic chemisorption may be ignored. Adsorption is examined in the region shown in Fig. 1.

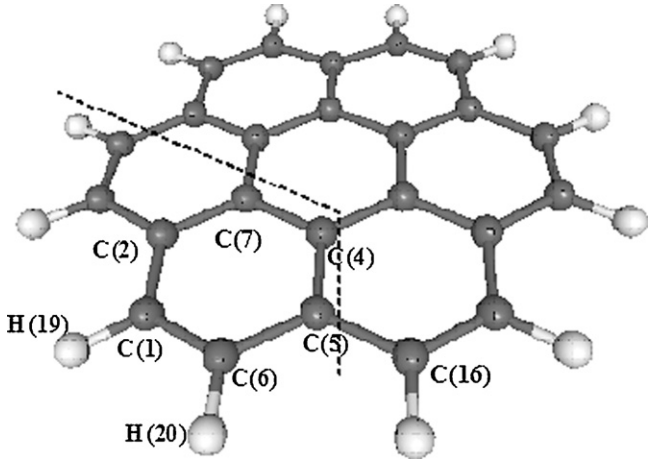

Fig. 1. Model PAH surface (coronene) with labelled carbon sites. The broken line indicates the region where H adsorption is tested.

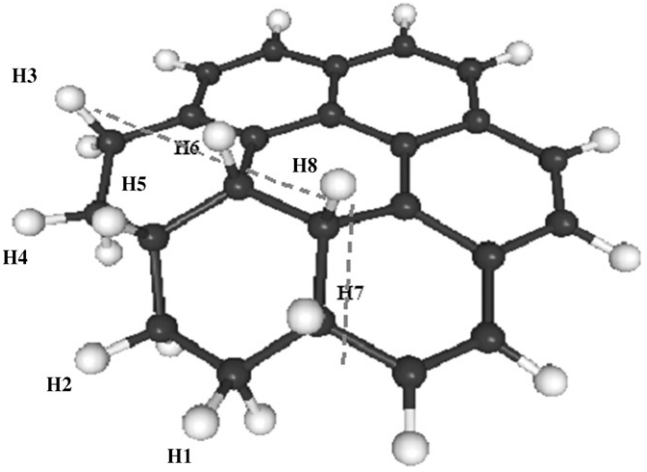

Fig. 2. Multiple hydrogen adsorption on the coronene surface (eight H atoms) labelled following their stability.

3. Results and discussion

We have carried out a detailed study of multiple hydrogen chemisorption and its effect on the graphitic surface as well as the molecular formation resulting from the interaction of atomic and molecular fragments with the surface covered by a hydrogen monolayer.

3.1. Multiple hydrogen chemisorption

Firstly, a single H atom chemisorption is analyzed in order to determine the preferential site. Allowing complete relaxation of surface model, a grid of calculations with a step of 0.5 Å is performed on the delimited region of the coronene surface shown in Fig. 1. Once the most stable adsorption site is found, a second H atom is added in order to find the next most stable site, and so forth. The most stable site for a single adsorption is on a surface edge atom with a complete system (adsorbate–substrate) spin multiplicity of $M = 2S + 1 = 2$ (see substrate site C(6) in Fig. 1 and H1 adsorbate in Fig. 2). For the second H adsorbate (H2), the most stable site is C(1), i.e. adjacent to the initial adsorption (see Figs. 1 and 2). Now $M = 1$ even though $M = 3$ is also feasible but energetically less favorable.

Preferential sites for the rest of the H adsorbates are also depicted in Fig. 2. They follow a similar pattern: adsorption on an edge atom followed by the corresponding adjacent site (see subsequent adsorbate pairs H3 + H4, H5 + H6 and H7 + H8). This is

Table 1
H adsorption on a coronene surface showing changes with coverage.

Coverage	E_{ad}	ϵ_{AB}	E_{AB}	W	r_{AB}	Charge
1H	−61.5	−0.412	−93.3	0.90	1.125	−0.04
2H	−57.8	−0.425	−96.7	0.94	1.125	−0.04
3H	−63.8	−0.413	−93.4	0.91	1.130	−0.04
4H	−53.6	−0.426	−96.8	0.94	1.122	−0.04
5H	−60.6	−0.406	−91.6	0.92	1.138	−0.06
6H	−51.1	−0.407	−90.8	0.92	1.138	−0.05
7H	−49.2	−0.400	−90.7	0.89	1.140	−0.05
8H	−42.3	−0.414	−90.4	0.94	1.125	−0.05

Adsorption energy (E_{ad}) and diatomic binding energy (E_{AB}) are given in kcal/mol, equilibrium bond distance (r_{AB}) in Å, and electric charge and diatomic energy (e_{AB}) in atomic units.

Table 2
H adsorption effects on coronene bond properties.

Bond	r_{AB}	E_{AB}	W
C(6)–H1	1.125 (–)	−93.3 (–)	0.90 (–)
C(6)–H(20)	1.116 (1.108)	−98.0 (−97.6)	0.94 (0.94)
C(6)–C(5)	1.508 (1.450)	−103.1 (−116.3)	0.97 (1.16)
C(6)–C(1)	1.481 (1.373)	−105.4 (−140.4)	1.00 (1.63)
C(5)–C(16)	1.428 (1.451)	−126.8 (−116.3)	1.28 (1.16)
C(5)–C(4)	1.464 (1.447)	−121.3 (−125.7)	1.21 (1.34)
C(1)–C(2)	1.414 (1.451)	−132.1 (−116.3)	1.34 (1.16)
C(1)–H(19)	1.070 (1.070)	−97.9 (−97.7)	0.94 (0.94)
H(20)–H1	1.746 (–)	2.2 (–)	0.00 (–)

Equilibrium bond distance (r_{AB}) and diatomic binding energy (E_{AB}) are given in Å and kcal/mol, respectively. Values in parentheses correspond to the bare surface.

explained by the fact that odd numbers of H create an unpaired electron adjacent to the adsorption site due to the breakage of a double bond, adsorption being thus favored on these sites. The most stable H atoms are thus located on the edge of the PAH compound (H1, H2, H3 and H4) in agreement with previous work [16]. Once edge sites are saturated, the inner sites are filled with the H5, H6, H7 and H8 atoms.

Values for the adsorption energy (E_{ad}), diatomic energy (ϵ_{AB}), diatomic binding energy (E_{AB}), Wiberg index (W), equilibrium bond distance (r_{AB}) and adsorbate charge as a function of substrate coverage are presented in Table 1. In general, E_{ad} and E_{AB} decrease with coverage. There also seems to be a correlation between ϵ_{AB}, W and E_{AB}: the smaller E_{AB}, the larger W and ϵ_{AB}. In all cases, H adsorption shows a small substrate to adsorbate electron transfer.

Our result for a single H adsorption of $E_{ad} = -61.5$ kcal/mol is in good accord with DFT values previously reported for positively charged naphthalene, anthracene, pyrene and coronene substrates [11,12], namely −63.3, −61.9, −61.4 and −56.1 kcal/mol. These results also agree with recent calculations of H adsorption on coronene$^+$ with DFT, PW91/DNP functionals and CATIVIC giving, respectively, −64.6, −61.7 and −60.8 kcal/mol [42]. Present E_{ad} for a single H atom on sites C(4) and C(5) (see Fig. 1) are respectively −46.6 and −46.9 kcal/mol. These results are also in relatively close agreement with those quoted in Ref. [12] of −35.7 and −40.5 kcal/mol, and show that adsorption is stronger on H-coordinated carbon atoms (carbon edge atoms) than on those surrounded by three carbon atoms; therefore, H_2 formation would be favored on the latter as will be shown in Section 3.4.

However, we find significant differences in adsorption energy with previous theoretical work: −13.1 kcal/mol [14], −17.3 kcal/mol [15] and −18.9 kcal/mol [20]. We have performed further DFT calculations of H adsorption on the C(1) (edge atom) and C(4) (central atom) sites of neutral coronene, obtaining respectively −34.7 and −17.1 kcal/mol. These results are in very good agreement with values estimated with the DMol^3 code (O. Castellano, private communications), and show that CATIVIC overestimates the adsorption energy with respect to DFT. In addition, by studying H adsorption on the basal plane (0 0 0 1) using periodic DFT with a pseudo-potential and the Perdew–Burke–Ernzerhof

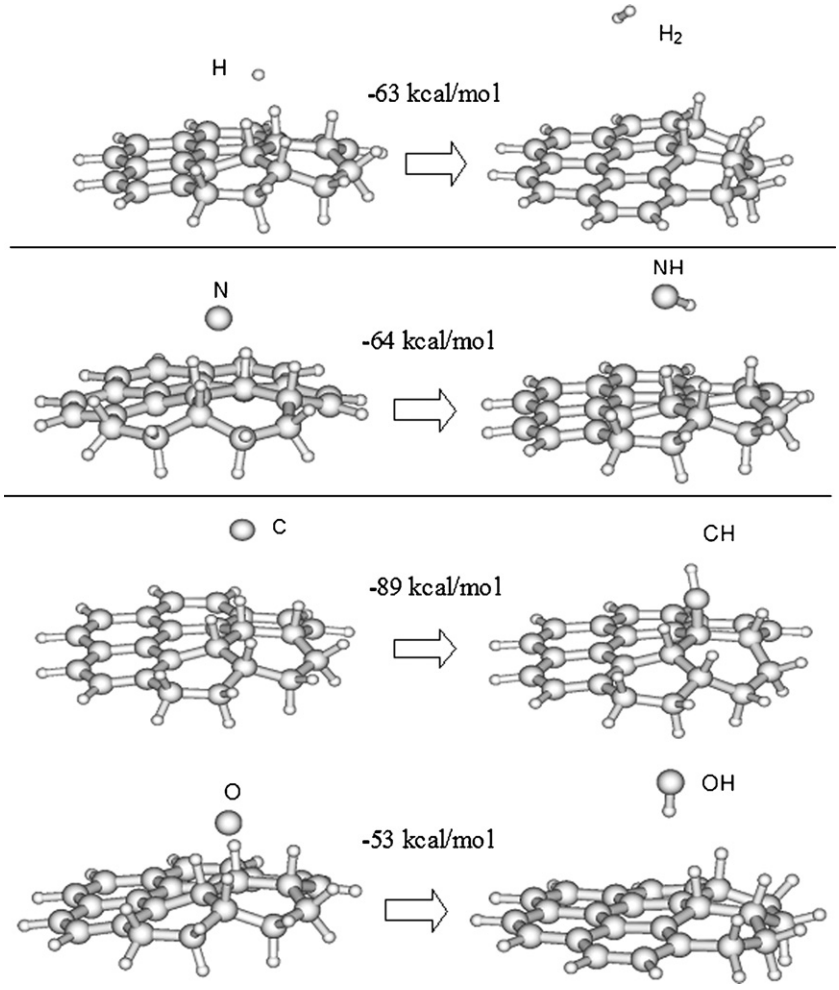

Fig. 3. Surface reactions of H, N, C and O on the coronene hydrogenated surface to form diatomic molecules.

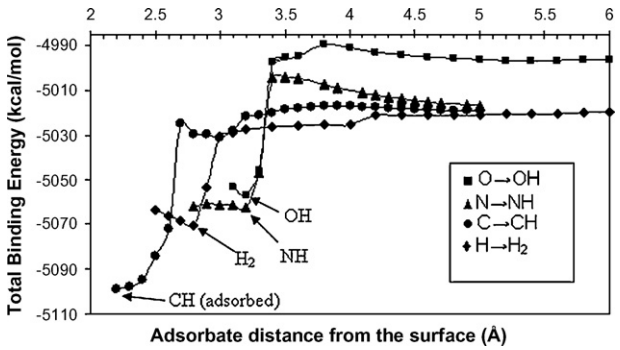

Fig. 4. Potential energy curves for H–H, H–N, H–C and H–O bond formation.

correlation functional [43], adsorption energy values very similar to this work (≈ −60 kcal/mol) have been obtained [21]. A close H adsorption energy of about −55 kcal/mol has also been reported [23]. Nevertheless, the adsorption gradient is in accord: adsorption on the edge is stronger than on a central site. Our calculated equilibrium bond distances (r_{AB}) of H above the surface C atom (1.122–1.140 Å) are very similar to those reported in the DFT calculations: 1.15 Å [14] and 1.129–1.141 Å [15].

3.2. Surface distortion due to H chemisorption

An analysis of E_{ad} as a function of adsorbate–substrate bond strength, evaluated in terms of E_{AB}, provides a measure of substrate reconstruction due to adsorption. For example, H1 adsorption on C(6) leads to $E_{ad} = -61.5$ kcal/mol and $E_{AB} = -93.3$ kcal/mol. This discrepancy of 31.8 kcal/mol may be explained by considering changes in the carbon lattice due to H adsorption. Local modifications (r_{AB}, E_{AB} and W) of the coronene surface atoms due to hydrogen adsorption are presented in Table 2. It is clear that H1 adsorption increases r_{AB} for atoms surrounding the adsorption site, namely C(1), C(5) and H(20) (see comparison between values with and without parentheses).

The local changes in the C(6)–C(5), C(6)–C(1) and C(6)–H(20) bonds (see Fig. 1) plus the H1–H(20) interaction are about $13.2 + 35.0 - 0.4 + 2.2 = 50.0$ kcal/mol. However, the first-neighbor bond strength involving the surrounding atoms (C(1)–H(19), C(1)–C(2), C(5)–C(16) and C(5)–C(4)) has stabilized ($-0.2 - 15.8 - 10.5 + 4.4 = -22.1$ kcal/mol). These two effects add up to a value of 27.9 kcal/mol which is close to the total destabilization caused by H1 adsorption (31.8 kcal/mol). Thus, H1 adsorption in general produces a distortion of the coronene surface with a bond-length enlargement for the first neighbors around the adsorption site and a shortening for the second neighbors (see values of r_{AB}, E_{AB} and W in Table 2).

A detailed study of surface distortion due to chemisorption of neutral H, CH_2 and CH_3 adsorbates on the coronene$^+$ system [42] yields a similar behavior: the region close to the adsorption site is destabilized while the rest of the system becomes more stable.

3.3. Formation of diatomic molecules

We assume that the graphitic surface is covered with a monolayer of H atoms. The interaction of H, O, C and N with the H covered surface seems to be a normal route for the formation of the OH, CH, NH and H_2 molecules; that is, the Eley–Rideal mechanism is considered for all surface reactions. In order to explore formation routes, a grid of calculations with a 0.5 Å step is again carried out. Different intermediates are found but priority is given to those leading to XH desorption from the coronene surface, X being either of the H, O, N and C incoming atoms. XH molecules are formed above a hydrogen atom (one-center), and because the H–C(4) bond strength is the weakest, a test site located perpendicular to C(4) on the hydro-

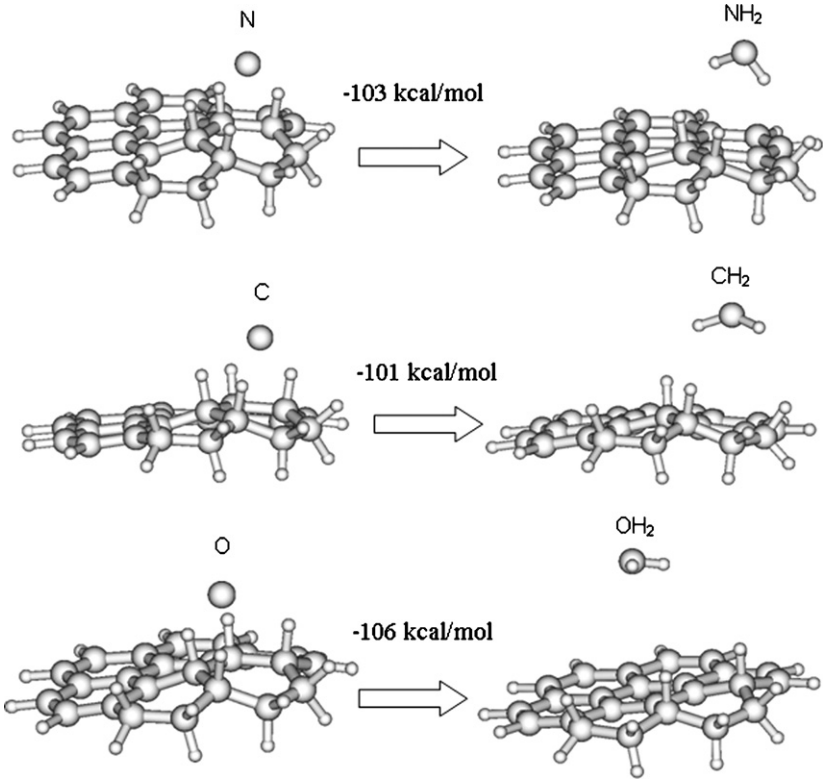

Fig. 5. Surface reactions of N, C and O on the coronene hydrogenated surface to form triatomic molecules.

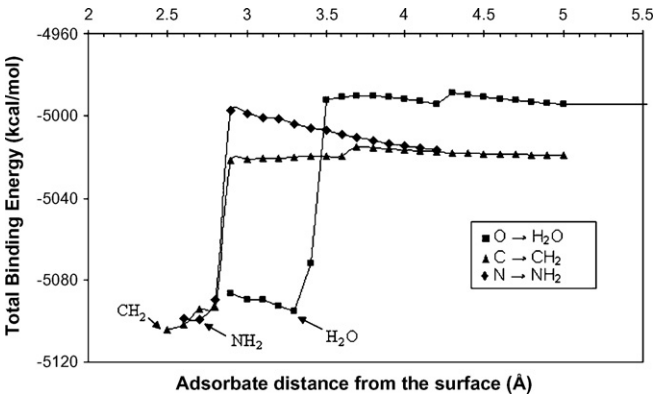

Fig. 6. Potential energy curves for NH_2, CH_2 and OH_2 formation.

genated surface is selected. Energy changes between the initial and final stages are shown in Fig. 3. The final stage is the result of full optimization after overcoming the reaction barrier that is outlined in the potential energy curve that is obtained. The incident atom (X) is able to abstract an H adsorbate in all cases except for C which becomes inserted in the surface C(4)–H bond. Energy changes due to the reaction

$$\text{surface} - H_n + X \rightarrow \text{surface} - H_{n-1} + XH \quad (4)$$

of −63, −64, −89 and −53 kcal/mol for H_2, NH, CH and OH, respectively, indicate that the formation of such diatomic molecules is thermodynamically feasible.

Facilities in CATIVIC allow the calculation of potential energy curves for the X–H interaction. The X–H distance is varied in steps of 0.1 Å starting at 5.0 Å, fixing the coordinates of X and the C atom to which the H atom is bonded. Thus, for each surface–X distance, the remaining atoms are optimized except for C(4) and X. Results shown in Fig. 4 indicate that, in most of the cases of XH molecular formation, it is required to surmount energy barriers except for H_2. For C–H, N–H and O–H, adsorption barriers are about 2, 12 and 7 kcal/mol, respectively. These results indicate that H_2 formation is favored with respect to other molecules following the order H_2 > CH > OH > NH. Note that during CH formation, a small well at about 3.0 Å from the surface is observed, which suggests the formation of a precursor state prior to the C(4)–CH insertion.

3.4. Formation of triatomic molecules

Triatomic molecules are also formed when X is located in the region around two adsorbed H atoms. Potential energy curves are obtained in the region between two H atoms adsorbed above C(4) and C(7) (see Fig. 1). Calculations at each point are carried out by fixing the *z* coordinate of C(4) and C(7) and all the coordinates of the X incoming species. A schematic representation of the surface reactions are presented in Fig. 5. Energy changes of −106, −103 and −101 kcal/mol for H_2O, NH_2 and CH_2, respectively, indicate that all reactions are thermodynamically possible. Potential energy curves (see Fig. 6) show barriers for XH_2 molecule formation of about 3, 7 and 20 kcal/mol for X = C, O and N, respectively. According to these qualitative results, formation of CH_2 at low temperatures is favored with respect to H_2O and NH_2. It is found that the strong surface–X bonding interactions, which lead to triatomic molecular formation, occur in a region 2.8–3.0 Å above the coronene surface.

3.5. Diatomic molecules on the hydrogenated surface

Once the formation of diatomic and triatomic molecules has taken place on the hydrogenated surface, it is interesting to follow further surface interactions. Because CH remains chemisorbed, as shown in Fig. 3, we then only analyze the surface reactions of OH and NH (see Fig. 7). The surface reaction is modeled by considering a hydrogen abstraction as the initial stage and the hydrogenated molecule as the final stage. As shown in Fig. 8, water synthesis occurs with the release of −82 kcal/mol over a barrier of about 20 kcal/mol. Depending on the spin state of NH, the interaction

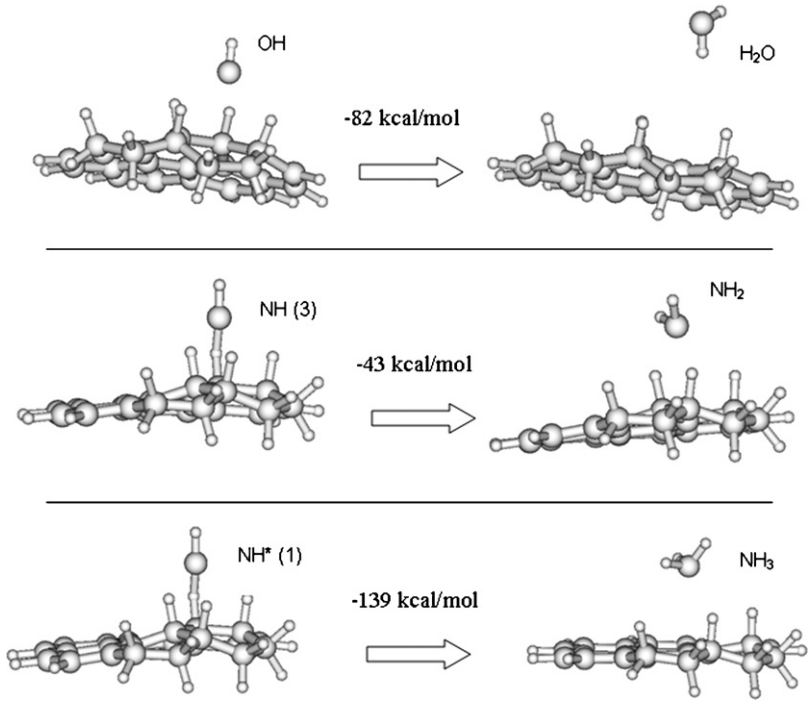

Fig. 7. Surface reactions for synthesis of H_2O, NH_2 and NH_3 from the interaction of OH and NH on hydrogenated coronene surface.

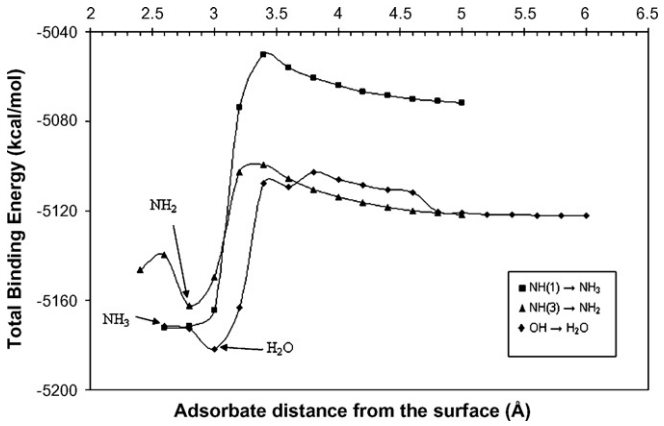

Fig. 8. Potential energy curves for the interaction of OH and NH with a hydrogenated coronene surface to form H_2O, NH_2 and NH_3.

with the hydrogenated surface yields the formation of either NH_2 or NH_3. Excited $NH^*(1)$ ($M = 1$) produces NH_3 with the release of −139 kcal/mol over a barrier of approximately 21 kcal/mol while NH(3) ($M = 3$) forms NH_2 with a reaction energy of −43 kcal/mol and a similar barrier to $NH^*(1)$.

3.6. Multiatomic molecules on the hydrogenated surface

Assembly of multiatomic molecules on the hydrogenated coronene surface is also possible (see Fig. 9). Triatomic molecules such as CH_2 and NH_2 lead to the synthesis of CH_3 and NH_3 with reaction energies of −71 and −50 kcal/mol, respectively, but surmounting barriers each of about 11 and 13 kcal/mol (see Fig. 10a). It must be pointed out that the NH_2 molecule has a long-range interaction minimum at about 4.0 Å that it is confirmed with a total optimization. Finally, methane formation also occurs when

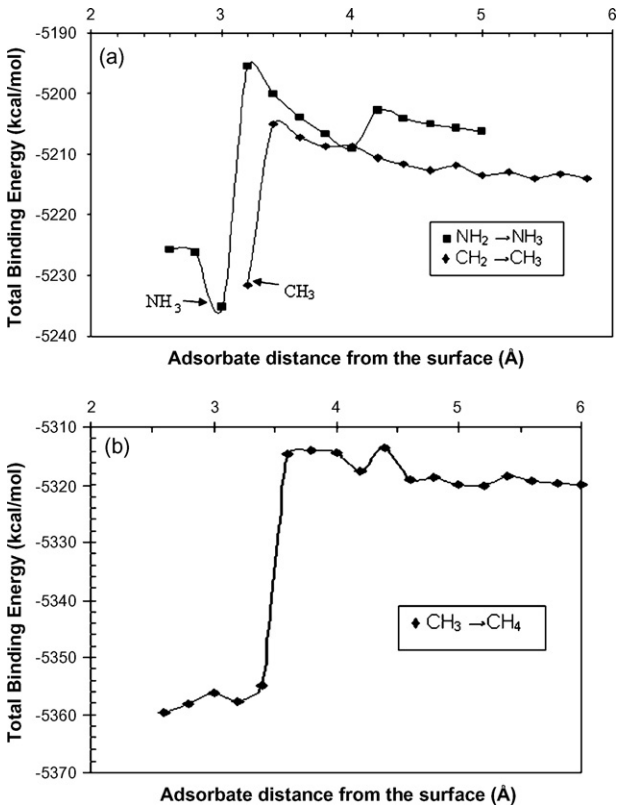

Fig. 10. Potential energy curves for formation of (a) NH_3 and CH_3 and (b) CH_4.

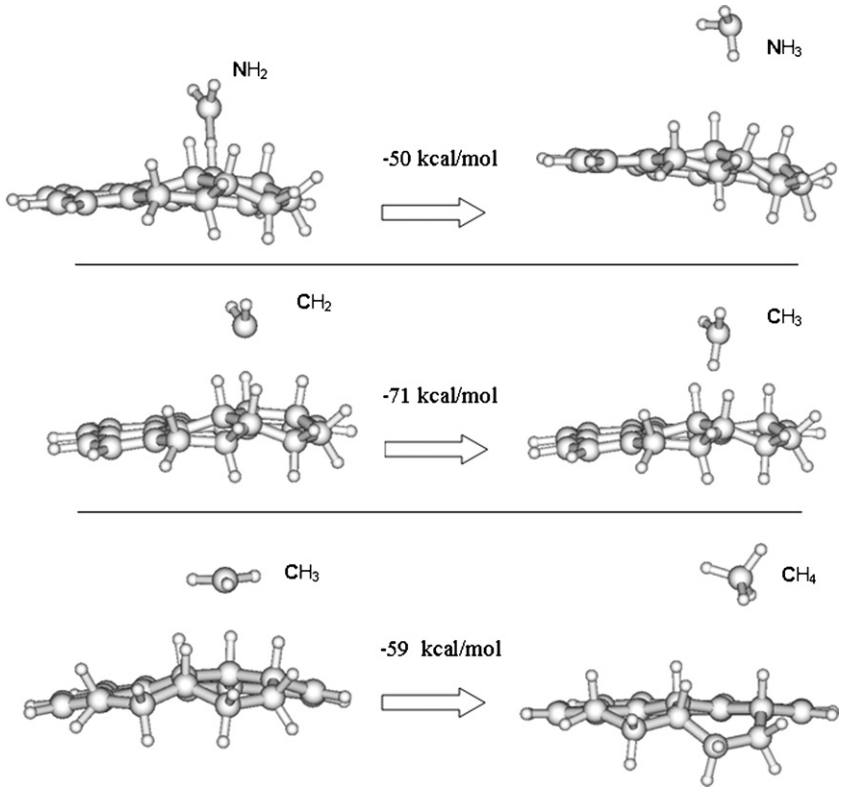

Fig. 9. Surface reactions of NH_2, CH_2 and CH_3 with a coronene hydrogenated surface. NH_3, CH_3 and CH_4 are respectively formed.

CH_3 interacts with the hydrogenated coronene surface and the system is stabilized at −59 kcal/mol; however, a small reaction barrier of about 6.5 kcal/mol has to be overcome (see Fig. 10b).

4. Conclusions and comments

Results of this work suggest that the use of a qualitative parametric method (CATIVIC) allows, in a simple way, the analysis of the formation processes of diatomic, triatomic and multiatomic molecules on a model surface. The most relevant findings of this work are as follows:

(a) The formation of an H monolayer on a coronene surface leads to significant distortion of the bond structure. Bond strength analysis of atomic H adsorption indicates that the surface is destabilized by about 32 kcal/mol. This is a trade-off between the destabilization of the nearest neighbors of the adsorption site and the bond stabilization that takes place in the rest of the coronene system. There is also an electronic charge transfer from the graphitic substrate to the H adsorbate.
(b) Molecular hydrogen formation occurs on the edge as well as on the central sites of the coronene cluster.
(c) The interaction of an incoming X atom (X = H, N, C and O) with a site directly around an H adsorbate leads to the formation of the H_2, NH, CH and OH molecules. All resulting molecules desorb from the surface except CH which remains chemisorbed to the surface.
(d) Interaction of X close to a bridge produces H_2O, NH_2 and CH_2 which desorb from the surface.
(e) Potential energy curves show barriers for the interaction of X with the surface, mainly for the case of the N and O atoms.
(f) Further surface reactions of di-, tri- and tetra-atomic radicals produce three-, four- and five-atom molecules since they are all thermodynamically favored. However, the paths of these radicals towards the surface involve reaction barriers, the smallest being that found in methane formation.
(g) Formation of di- and tri-atomic molecules from incoming X atoms are important inasmuch as they are precursors for the formation of more complex organic molecules, e.g. amino acids, alcohols, sugar, polyols, etc. Therefore, more work is planned to study different surface reactions, taking into account the Langmuir–Hinshelwood mechanism that imply the calculation of migration barriers and transition states for the formation of different species on the surface. In addition, Eley–Rideal abstraction may also occur starting from intermediates of the type XH_n ($n = 1 - 3$ and X = O, N and C) adsorbed on the surface and the interaction with molecular fragments such as $X'H_m$ ($m = 1 - 3$) to produce $XX'H_{m+n}$.

Acknowledgements

We gratefully acknowledge support from FONACIT (Venezuela) under the contract G-97000667 and, more recently, from the LOCTI research program. We also thank María Cristina Goite for help in the initial steps of this calculation and Yenner Betancurt and Alexander Peraza for ideas referring to the screening codes.

References

[1] W.F. Huebner, L.E. Snyder, in: P.J. Thomas, R.D. Hicks, C.F. Chyba, C.P. McKay (Eds.), Comets and the Origin and Evolution of Life, Advances in Astrobiology and Biogeophysics, Springer, 2006, p. 113.
[2] E. Dweck, R.G. Arendt, D.J. Fixsen, T.J. Sodroski, N. Odegard, J.L. Weiland, W.T. Reach, M.G. Hauser, T. Kelsall, S.H. Moseley, R.F. Silverberg, R.A. Shafer, J. Ballester, D. Bazell, R. Isaacman, Astrophys. J. 475 (1997) 565.
[3] A.J. Bennett, B. McCarroll, R.P. Messmer, Surf. Sci. 24 (1971) 191.
[4] R. Dovesi, C. Pisani, F. Ricca, C. Roetti, J. Chem. Phys. 65 (1976) 4116.
[5] R. Dovesi, C. Pisani, F. Ricca, C. Roetti, Surf. Sci. 72 (1978) 140.
[6] J.P. Chen, R.T. Yang, Surf. Sci. 216 (1989) 481.
[7] C. Mendoza, F. Ruette, Catal. Lett. 3 (1989) 89.
[8] E. Habart, F. Boulanger, L. Verstraete, C.M. Walmsley, G. Pineau des Forêts, Astron. Astrophys. 414 (2004) 531.
[9] T. Velusamy, W.D. Langer, Astronom. J. 136 (2008) 602.
[10] C.W. Bauschlicher, Astrophys. J. 509 (1998) L125.
[11] M. Hirama, T. Ishida, J.-I. Aihara, J. Comput. Chem. 24 (2003) 1378.
[12] M. Hirama, T. Tokosumi, T. Ishida, J.-I. Aihara, Chem. Phys. 305 (2004) 307.
[13] T. Fromherz, C. Mendoza, F. Ruette, Mon. Not. R. Astron. Soc. 263 (1993) 851.
[14] L. Jeloaica, V. Sidis, Chem. Phys. Lett. 300 (1999) 157.
[15] Y. Ferro, F. Marinelli, A. Allouche, J. Chem. Phys. 116 (2002) 8124.
[16] T. Zecho, A. Güttler, X. Sha, B. Jackson, J. Küppers, J. Chem. Phys. 117 (2002) 8486.
[17] X. Sha, B. Jackson, Surf. Sci. 496 (2002) 318.
[18] Y. Ferro, F. Marinelli, A. Allouche, Chem. Phys. Lett. 368 (2003) 609.
[19] S. Morisset, F. Aguillon, M. Sizun, V. Sidis, Chem. Phys. Lett. 378 (2003) 615.
[20] L. Hornekær, E. Rauls, W. Xu, Ž. Šljivančanin, R. Otero, I. Stensgaard, E. Lægsgaard, B. Hammer, F. Besenbacher, Phys. Rev. Lett. 97 (2006) 186102.
[21] A. Allouche, A. Jelea, F. Marinelli, Y. Ferro, Phys. Scr. T124 (2006) 91.
[22] D. Bachellerie, M. Sizun, D. Teillet-Billy, N. Rougeau, V. Sidis, Chem. Phys. Lett. 448 (2007) 223.
[23] T. Roman, W.A. Diño, H. Nakanishi, H. Kasai, T. Sugimoto, K. Tange, Carbon 45 (2007) 203.
[24] Y. Ferro, D. Teillet-Billy, N. Rougeau, V. Sidis, S. Morisset, A. Allouche, Phys. Rev. B 78 (2008) 085417.
[25] E. Rauls, L. Hornekær, Astrophys. J. 679 (2008) 531.
[26] S. Casolo, O.M. Løvvik, R. Martinazzo, G.F. Tantardini, J. Chem. Phys. 130 (2009) 0504704.
[27] C. Mendoza, F. Ruette, G. Martorell, L.S. Rodríguez, Astrophys. J. 601 (2004) L59.
[28] C. Mendoza, L.S. Rodríguez, F. Ruette, S. Schnell, Surf. Sci. 602 (2008) 1053.
[29] D.M. Mehringer, L.E. Snyder, Y. Miao, F.J. Lovas, Astrophys. J. 480 (1997) L71.
[30] J.M. Hollis, F.J. Lovas, P.R. Jewell, Astrophys. J. 540 (2000) L107.
[31] Y.-J. Kuan, S.B. Charnley, H.-C. Huang, W.-L. Tseng, Z. Kisiel, Astrophys. J. 593 (2003) 848.
[32] F. Ruette, M. Sánchez, G. Martorell, C. González, R. Añez, A. Sierraalta, L. Rincón, C. Mendoza, Int. J. Quant. Chem. 96 (2004) 321.
[33] F. Ruette, M. Sánchez, C. Mendoza, A. Sierraalta, G. Martorell, C. González, Int. J. Quant. Chem. 96 (2004) 303.
[34] R. Martínez, F. Brito, M.L. Araujo, F. Ruette, A. Sierraalta, Int. J. Quant. Chem. 97 (2004) 854.
[35] J.R. Primera, M. Sánchez, M. Romero, A. Sierraalta, F. Ruette, J. Mol. Struct. (Theochem) 469 (1999) 177.
[36] M. Romero, M. Sánchez, A. Sierraalta, L. Rincón, F. Ruette, J. Chem. Inf. Comput. Sci. 39 (1999) 543.
[37] G. Blyholder, J. Head, F. Ruette, Theor. Chim. Acta 60 (1982) 429.
[38] R.C. Bingham, M.J.S. Dewar, D.H. Lo, J. Am. Chem. Soc. 97 (1975) 1285.
[39] F. Ruette, F.M. Poveda, A. Sierraalta, J. Rivero, Surf. Sci. 349 (1996) 241.
[40] R. Saija, M.A. Iati, F. Borghese, P. Denti, S. Aiello, C. Cecchi-Pestellini, Astrophys. J. 559 (2001) 993.
[41] J. Rodríguez, J. Sánchez-Marín, F. Torrens, F. Ruette, J. Mol. Struct. (Theochem) 254 (1992) 429.
[42] F. Ruette, M. Sánchez, O. Castellano, H. Soscún, Int. J. Quantum Chem., in press.
[43] J.P. Perdew, K. Burke, M. Ernzerhof, Phys. Rew. Lett. 77 (1996) 3865.